International Journal of Multiphase Flow 35 (2009) 307–311

Contents lists available at ScienceDirect

International Journal of Multiphase Flow

journal homepage: www.elsevier.com/locate/ijmulflow

Galilean invariance in the lattice-Boltzmann method and its effect on the calculation of rheological properties in suspensions

Jonathan R. Clausen, Cyrus K. Aidun *

Department of Mechanical Engineering, Georgia Institute of Technology, 500 10th Street NW, Atlanta, GA 30318, USA

ARTICLE INFO

Article history:
Received 20 November 2008
Accepted 18 January 2009
Available online 7 February 2009

ABSTRACT

The lattice-Boltzmann method (LBM) provides an efficient simulation technique for the study of particle suspensions. These simulations provide an important tool in elucidating the effect of suspended particles on the rheology of suspensions. The most common solid–fluid boundary condition used in the LBM is the bounce-back operation, and as such, the errors introduced by this operation to the dynamics of the particles and the calculation of relevant rheological quantities must be quantified. This paper derives the Galilean invariant term in the standard bounce-back operation and shows the effect of this error on the calculation of particle dynamics and stresslet. In particular, an error is found in the calculation of normal stresses that may be significant in magnitude compared with typical values found in suspensions of rigid spherical particles. A correction is proposed, and simulation results are shown that verify the original assessment and show the reduction of error when using the proposed correction.

1. Introduction

Understanding the rheology of particle suspensions is important in many industrial and biological fields and can lead to advancements in the handling of slurries, coating and fiber flows in the paper-making process, and in biological flows such as blood. Analytical tools are typically constrained to the dilute limit (Einstein, 1906; Batchelor and Green, 1972) or in the form of semi-empirical relationships that do not fully account for the non-Newtonian effects seen at higher concentrations (Krieger and Dougherty, 1959). Experimental studies of normal stresses in non-colloidal suspensions of rigid spheres exist for higher concentrations (Zarraga et al., 2000; Singh and Nott, 2003); however, the small magnitude of these stresses makes accurate measurements difficult at lower concentrations. As a result, numerical simulations have proved instrumental in advancing our understanding of suspension rheology. In particular, Stokesian dynamics has highlighted the connection between microstructure and normal stresses causing non-Newtonian behavior (Phung et al., 1996; Sierou and Brady, 2002), as well as the diffusive nature found in non-colloidal suspensions (Sierou and Brady, 2004). However, Stokesian dynamics does have shortcomings such as being constrained to the Stokes flow limit and limited to spherical particles. The lattice-Boltzmann method (LBM) outlined in Section 2 allows for the efficient simulation of particle suspensions and is capable of simulating complex particle shapes at finite Reynolds numbers. Additionally, the local nature of the LBM allows for significant parallelism resulting in excellent scaling on distributed memory clusters. Increasingly, the LBM has been used for calculating rheological properties such as shear viscosity and normal stresses (Kulkarni and Morris, 2008; MacMeccan et al., 2009). It is well known that the LBM approximates the incompressible Navier–Stokes equations with compressibility errors that grow as M^2, where M is the LBM Mach number. It is also known that the LBM is Galilean invariant with errors of $O(u^3)$, where u is the magnitude of fluid velocity, and the Mach number is related to the velocity through the LBM pseudo-sound-speed, c_s, by $M = u/c_s$. This has led to the typical statement that simulations with $M \leqslant 0.1$ result in negligible error, which is appropriate in many cases. However, the recent interest in more sensitive parameters such as normal stress differences, suspension pressures, and particle diffusivity indicates that these errors may be important. The effect of these errors on the calculation of the particle stresslet is especially important. In this paper, the Galilean error in the LBM bounce-back and its effect on particle dynamics and stresslet calculations are quantified, and a correction is proposed.

2. Lattice-Boltzmann method

The lattice-Boltzmann method is the evolution of lattice-gas automata, in which additional averaging is used to smooth the statistical fluctuations inherent in lattice-gas simulations. Early in the application of the LBM to particle suspensions, two major variants were developed. The first simulates particles as shells with an internal fluid (Ladd, 1994a,b), and the second simulates particles as solid objects with a virtual fluid that has no impact on particle dynamics (Aidun and Lu, 1995; Aidun et al., 1998). Both methods

* Corresponding author. Tel.: +1 404 894 6645; fax: +1 404 894 4778.
E-mail address: cyrus.aidun@me.gatech.edu (C.K. Aidun).

0301-9322/$ - see front matter © 2009 Elsevier Ltd. All rights reserved.
doi:10.1016/j.ijmultiphaseflow.2009.01.007

give accurate results for non-colloidal suspensions where inertial lag is not important (Heemels et al., 2000), and the relative merits of each method have been covered (Ladd and Verberg, 2001); however, important differences appear when looking at errors causing Galilean invariance.

In the LBM, the Boltzmann equation is discretized in velocity space in terms of lattice velocity vectors, $\mathbf{e}_i$, which results in the creation of lattice nodes found at Cartesian positions, $\mathbf{r}$. At each lattice node, a distribution of fluid particles f_i exists for every lattice direction, where the index i refers to the lattice direction. The time evolution of these distributions is governed by subsequent collision and streaming operations. In the case of the widely used single-relaxation-time linear collision operator, the update can be expressed as

$$f_i(\mathbf{r}+\mathbf{e}_i, t+1) = f_i(\mathbf{r}, t) - \frac{1}{\tau}\left(f_i(\mathbf{r}, t) - f_i^{(eq)}(\mathbf{r}, t)\right), \tag{1}$$

where $f_i^{(eq)}(\mathbf{r}, t)$ is the equilibrium distribution function, and the collision operation is related to the fluid viscosity by $\tau = \nu/c_s^2 + 1/2$. It is important to note that the issues discussed here are also applicable to the more general collision operators. Macroscopic fluid variables are recovered through moments of the distribution function, shown as

$$\sum_i f_i(\mathbf{r}, t) = \rho \quad \sum_i f_i(\mathbf{r}, t)\mathbf{e}_i = \rho\mathbf{u} \quad \sum_i f_i(\mathbf{r}, t)\mathbf{e}_i\mathbf{e}_i = c_s^2\rho\mathbf{I} + \rho\mathbf{u}\mathbf{u}, \tag{2}$$

where ρ is the fluid density and $\mathbf{u}$ is the fluid velocity. The most common variants are the D2Q9, for 2-dimensional 9-velocity, and D3Q19, for 3-dimensional 19-velocity, models. The equilibrium distribution is calculated as a function of the macroscopic fluid variables ρ and $\mathbf{u}$, which are related to the fluid distribution through moments in (2). The equilibrium distribution is expressed as

$$f_i^{(eq)} = w_i\rho\left[1 + \frac{1}{c_s^2}(\mathbf{e}_i\cdot\mathbf{u}) + \frac{1}{2c_s^4}(\mathbf{e}_i\cdot\mathbf{u})^2 - \frac{1}{2c_s^2}u^2\right]. \tag{3}$$

For the D2Q9 model, values for w_i are 4/9 for the rest direction, 1/9 for the non-diagonal directions, and 1/36 for the diagonal directions. For the D3Q19 model, values for w_i are 1/3, 1/18, and 1/36 for the rest, non-diagonal, and diagonal directions, respectively. The pseudo-sound-speed, c_s, is $\sqrt{1/3}$ in both cases, and this value will be used hereafter.

The LBM fluid and solid particle are coupled through a moving-boundary bounce-back condition. The momentum of the fluid distribution adjacent to a moving boundary is adjusted according to

$$f_i(\mathbf{r}, t+1) = f_{i'}(\mathbf{r}, t^+) + 6\rho w_i\mathbf{u}_b\cdot\mathbf{e}_i \tag{4}$$

for a boundary link (BL) in the i' direction, where i' is the direction opposite of i, and t^+ denotes the time post collision but prior to streaming in (1). Assuming a time step of one and uniform distribution of force over a single time step, the adjustment in (4) corresponds to a traction force on the object of

$$\mathbf{F}_{i'}^{(b)}\left(\mathbf{r}+\frac{1}{2}\mathbf{e}_{i'}, t\right) = -2\mathbf{e}_i[f_{i'}(\mathbf{r}, t^+) + 3\rho w_i\mathbf{u}_b\cdot\mathbf{e}_i]. \tag{5}$$

Total force and torque are given by summations over all boundary links according to

$$\mathbf{F} = \sum_{BL}\mathbf{F}_{i'}^{(b)}\left(\mathbf{r}+\frac{1}{2}\mathbf{e}_{i'}, t\right) \tag{6}$$

$$\mathbf{T} = \sum_{BL}\left(\mathbf{r}+\frac{1}{2}\mathbf{e}_{i'} - \mathbf{r}_0\right)\times\mathbf{F}_{i'}^{(b)}\left(\mathbf{r}+\frac{1}{2}\mathbf{e}_{i'}, t\right), \tag{7}$$

where $\mathbf{r}_0$ is the particle's center of mass. Particle dynamics are calculated using Newtonian mechanics. Typical schemes include explicit integration (Aidun et al., 1998; Ding and Aidun, 2003) and implicit integration (Nguyen and Ladd, 2002).

3. Analysis

3.1. Calculation of error term

To calculate Galilean errors, consider a moving boundary adjacent to a fluid node as depicted in Fig. 1. A fluid node adjacent to a solid surface is called a fluid boundary node (FBN), and the point of force application, which is the midpoint on the boundary link, is called the mid node. In a fully relaxed system in which the mesh size tends to zero, the FBNs relax to an equilibrium distribution approaching the boundary velocity, $\mathbf{u}_b$, and no force should be applied on the boundary. Calculating the equilibrium distribution using the boundary velocity with (3) and substituting into (5) results in an error term given by

$$\mathbf{F}_{i'}^{(err)} = -2\rho w_i\mathbf{e}_i\left[1 + \frac{9}{2}(\mathbf{e}_i\cdot\mathbf{u}_b)^2 - \frac{3}{2}u_b^2\right]. \tag{8}$$

Clearly, the quadratic terms in the equilibrium distribution break Galilean invariance. It is important to note that when simulating fluid-filled shells, there exists a corresponding internal fluid node which exactly cancels the error present in (8); therefore, no error in particle force and torque exists. When simulating a solid particle, however, the internal fluid has no impact on particle dynamics, thus global errors in force and torque calculations may exist. Both methods have errors in external traction vector calculations typically used in the calculation of the particle contribution to suspension stress.

3.2. Correction

The Galilean error in (8) can be canceled by creating an internal boundary node (IBN) with a distribution set to $f_i^{(eq)}(\rho, \mathbf{u}_b)$ at every link endpoint inside the particle, as shown in Fig. 1. The distributions from the IBNs then undergo the normal bounce-back operation, and the force is applied to the particle exactly canceling the error terms (MacMeccan, 2007, pp. 57–61). The equilibrium distribution in these internal nodes can be calculated in a link-by-link manner and only in the necessary directions for computational efficiency. Recently, Caiazzo and Junk (2008) have analyzed the bounce-back operation using a diffusive scaling for the LBM (Junk et al., 2005) and recovered an identical error term. They propose a corrected bounce-back operation by subtracting (8) from (5) directly. Both methods are equivalent.

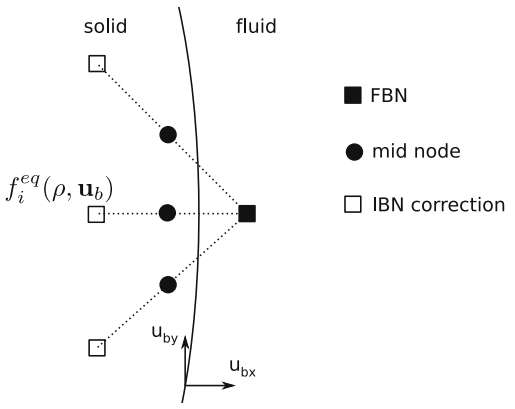

Fig. 1. Fully relaxed fluid node adjacent to a moving boundary, referred to as a fluid boundary node (FBN). Boundary links shown crossing solid boundary.

In order to gauge the impact of this link-wise error, first estimate the effect of one FBN by adding the errors from all boundary links crossing the surface. Eliminating discretization effects, the boundary velocity for all links emanating from the same FBN will be equal. For the vertical wall shown in Fig. 1 with a D2Q9 LBM scheme, the errors from (8) are summed to result in

$$\mathbf{F}_{FBN}^{(err)} = -\rho \begin{bmatrix} 1/3 + u_{bx}^2 \\ u_{bx}u_{by} \end{bmatrix}, \tag{9}$$

where u_{bx} and u_{by} are the x and y components of the boundary velocity. Also note that the length of the surface described by one FBN is a single lattice unit making the expression in (9) equivalent to a stress. A similar analysis can be performed for a horizontal wall, and the results can be generalized to handle either side of the wall via the boundary normal vector, $\mathbf{n}$. The resulting error terms, designated with V and H for vertical and horizontal, are

$$\mathbf{F}_{FBN-V}^{(err)} = -\rho \frac{n_x}{|n_x|} \begin{bmatrix} 1/3 + u_{bx}^2 \\ u_{bx}u_{by} \end{bmatrix}, \quad \mathbf{F}_{FBN-H}^{(err)} = -\rho \frac{n_y}{|n_y|} \begin{bmatrix} u_{bx}u_{by} \\ 1/3 + u_{by}^2 \end{bmatrix}. \tag{10}$$

The goal is to extend the discrete results from (10) to arbitrarily oriented surfaces in a continuous fashion. In the LBM, a smooth object is represented by mid nodes that reside on the midpoint of links crossing the solid surface, as illustrated in Fig. 2. This discretization results in a stair-stepping effect such that an inclined surface is represented by a combination of vertical and horizontal surfaces. Thus, for an arbitrarily oriented surface, the error can be approximated as a combination of errors from both horizontal and vertical surfaces, with appropriate weighting for the projected area. Such an assumption also agrees with the isotropic structure of the lattice. Thus, the boundary force on an arbitrarily aligned surface element can be expressed as

$$\delta\mathbf{F}^{(err)} = |n_x|\mathbf{F}_{FBN-V}^{(err)} + |n_y|\mathbf{F}_{FBN-H}^{(err)}, \tag{11}$$

which can be simplified to

$$\delta\mathbf{F}^{(err)} = -\rho \begin{bmatrix} n_x\left(1/3 + u_{bx}^2\right) + n_y u_{bx}u_{by} \\ n_y\left(1/3 + u_{by}^2\right) + n_x u_{bx}u_{by} \end{bmatrix}. \tag{12}$$

A similar analysis can be performed for the D3Q19 lattice model, and the error in boundary force can be described as

$$\delta\mathbf{F}^{(err)} = -\rho \begin{bmatrix} n_x\left(1/3 + u_{bx}^2\right) + n_y u_{bx}u_{by} + n_z u_{bx}u_{bz} \\ n_y\left(1/3 + u_{by}^2\right) + n_x u_{bx}u_{by} + n_z u_{by}u_{bz} \\ n_z\left(1/3 + u_{bz}^2\right) + n_x u_{bx}u_{bz} + n_y u_{by}u_{bz} \end{bmatrix}. \tag{13}$$

In both 2-dimensional and 3-dimensional cases, the normal forces created by the Galilean error can be expressed as

$$\delta\mathbf{F}^{(err)} \cdot \mathbf{n} = -\rho\left[1/3 + (\mathbf{u}_b \cdot \mathbf{n})^2\right]. \tag{14}$$

The first term is simply the hydrostatic pressure found in the LBM, where $P = c_s^2\rho$, and can typically be neglected. The second term breaks Galilean invariance and creates errors in normal stresses that scale as u^2.

3.3. Effect on rheology calculations

By inspection, (14) creates an artificial normal stress on the fore and aft surface of a translating particle. Quantifying the impact of the normal error on the calculation of total force and particle stresslet is found by integrating over the differential error. The stresslet is simply a measure quantifying the effect of a suspended particle on the average stress in the suspension. In terms of particle stresslet, $\mathbf{S}$, the volume-averaged stress in a 3-dimensional suspension can be expressed as

$$\boldsymbol{\Sigma} = -P\mathbf{I} + 2\mu\mathbf{E} + \frac{1}{V}\sum \mathbf{S}, \tag{15}$$

where $\boldsymbol{\Sigma}$ is the average stress in the suspension, P is the mean fluid pressure, $\mathbf{E}$ is the average rate-of-strain tensor, V is the domain volume, and μ is the suspending fluid viscosity (Batchelor, 1970). The summation is over all particles in the domain. The force and stresslet errors are calculated by integrating on the particle surface, Γ, shown as

$$\mathbf{F}^{(err)} = \int \delta\mathbf{F}^{(err)} d\Gamma \tag{16}$$

for the error in total force on the particle, and

$$\mathbf{S}^{(err)} = \int \frac{1}{2}\left(\delta\mathbf{F}^{(err)}\mathbf{x} + \mathbf{x}\delta\mathbf{F}^{(err)}\right) d\Gamma \tag{17}$$

for the error in particle stresslet, where $\mathbf{x}$ is a vector from the center of the particle to the surface. Consider a spherical particle in simple shear in which the particle is traveling with the local fluid velocity, U_x, and rotating with the local rotation of the fluid, $\dot{\gamma}/2$, where $\dot{\gamma}$ is the shear rate. Such situations frequently arise during simulations, such as a particle in simple shear near a domain wall, as shown in Fig. 3. Calculating the integrals in (16) and (17) with the appropriate boundary velocity and neglecting the isotropic static pressure results in error terms of

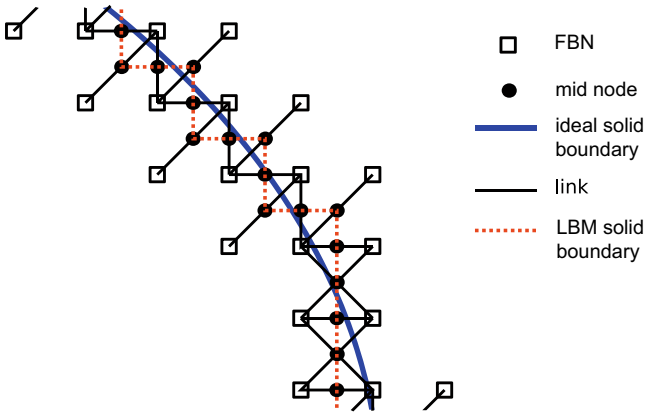

Fig. 2. Discretization of smooth particle by links crossing particle boundary creating a combination of horizontal and vertical surfaces. Actual particle boundary shown by heavy blue line, and particle boundary as seen by the LBM shown by dotted red line. Applying proposed correction would put IBNs at all link endpoints within the particle (not shown).

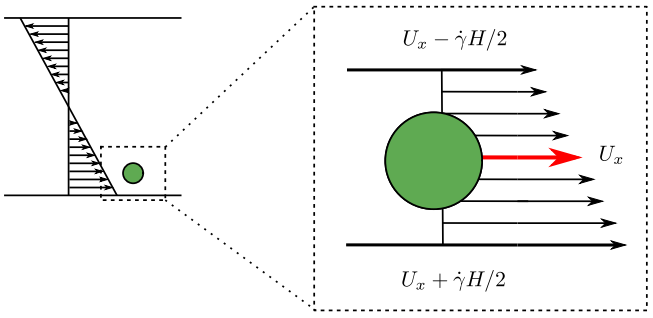

Fig. 3. Particle in simple shear near the domain border in a large-scale simulation is analogous to a particle with superposed shear and translational velocity.

$$F_y^{(err)} = -\rho V_p \dot{\gamma} U_x/2 \tag{18}$$

and

$$S_{11}^{(err)} = -\rho V_p U_x^2, \tag{19}$$

where V_p is the volume of the particle. All other force and stresslet errors are zero. Substituting the error terms into (15) gives an idea of the suspension-level impact, as the error in suspension stress can be written as

$$\Sigma_{11}^{(err)} = -\rho\phi U_x^2, \tag{20}$$

where ϕ is the volume (or areal) fraction of the suspended phase. It is worth mentioning that the suspension stress calculation neglects inertial terms that may need to be present in addition to the stresslet at finite Reynolds number; however, the purpose of this study is to demonstrate the error in the stresslet calculation. Galilean errors are independent of Reynolds number, since Galilean shifts do not necessarily change the particle Reynolds number, defined as $Re_p = \rho\dot{\gamma}R^2/\mu$ where R is the particle radius. For suspensions of rigid spheres, normal stresses are small at low concentrations ($\leqslant 20\%$), with magnitudes of $O(10^{-2})$ when normalized by $\mu\dot{\gamma}$ (Sierou and Brady, 2002). At these small magnitudes, errors in (20) may be significant. The correction described in Section 3.2 can eliminate these errors.

3.4. Simulations

The simplest test case is a sphere suspended centered in a wall-bounded domain, in which the fluid, walls, and sphere have the same translational velocity. Physically, this is equivalent to a stationary sphere in a quiescent fluid. Such a case does not result in a force error since $\dot{\gamma} = 0$; however, it does result in an error in the stresslet calculation. Fig. 4 shows the stresslet error as a function of translational velocity, and the results scale as U_x^2. The results for the corrected bounce-back are not shown, but errors are $O(10^{-11})$ or less in all cases. Inset in the figure is a graphic of the particle showing the normal stress on the particle's surface, where warm colors denote high stress areas (color online). The simulation domain is $64 \times 64 \times 64$ lattice nodes, and the particle has a radius of 10 lattice nodes, but the results are insensitive to domain size since the fluid distributions never depart from equilibrium. A net force of zero is recorded in all cases as predicted by (18) (not shown).

Next, a sphere is suspended centered in wall-bounded shear such that it rotates and translates, as shown on the right side of Fig. 3. An error in the y-component of total force that increases linearly with both the shear rate and translational velocity is shown in the dependence of force on $U_x\dot{\gamma}$ in (18). These simulations measure the error in force directly by fixing the sphere in the y-direction only. All other degrees of freedom in motion are allowed. For the 3-dimensional simulation shown, the domain is $64 \times 128 \times 64$ lattice nodes, with a particle radius of 10 lattice nodes. The top and bottom wall are initialized to $U_x - \dot{\gamma}H/2$ and $U_x + \dot{\gamma}H/2$, respectively, where H is the domain height. Results for the y-component of force are shown in Fig. 5(a,b) for fluid-filled particles, solid particles with corrected and uncorrected bounce-back operations, and the analytic predictions. Also shown are results for the external boundary force (EBF) method (Wu and Aidun, in press), which is not based on the bounce-back procedure and thus does not display Galilean errors. In Fig. 5a the translational velocity is held constant while the shear rate is altered, and in Fig. 5b the shear rate is held constant while the translational velocity is altered. The force error shows a linear dependence on $U_x\dot{\gamma}$ in both cases, as predicted by (18). A slight drift occurs in the results, especially in Fig. 5b where the translational velocity is increased. One possible explanation is the compressibility error which scales as U_x^2. Although the Galilean invariant portion of the error is corrected, compressibility artifacts still exist at high Mach number. Another possible source of error is the finite discretization of the particle. Nevertheless, the predicted scaling in the error term is demonstrated. Stresslet results agree with the scaling in (19) and echo the findings in Fig. 4.

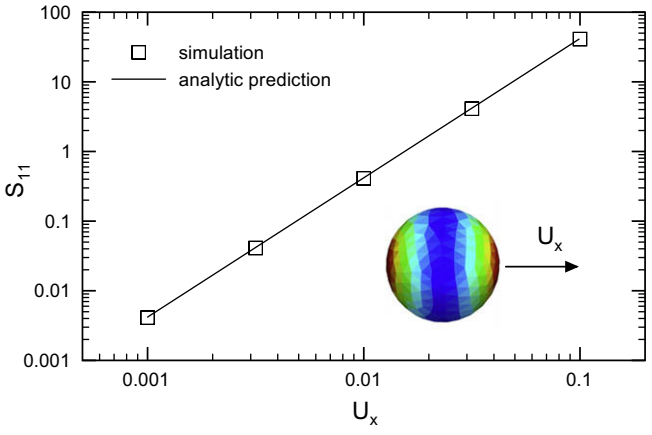

Fig. 4. Effect of translational velocity on S_{11}. Inset in figure is a graphical depiction of exaggerated normal stresses on fore and aft surfaces of sphere. Not shown are results with the corrected bounce-back showing $O(10^{-11})$ error or less in all cases.

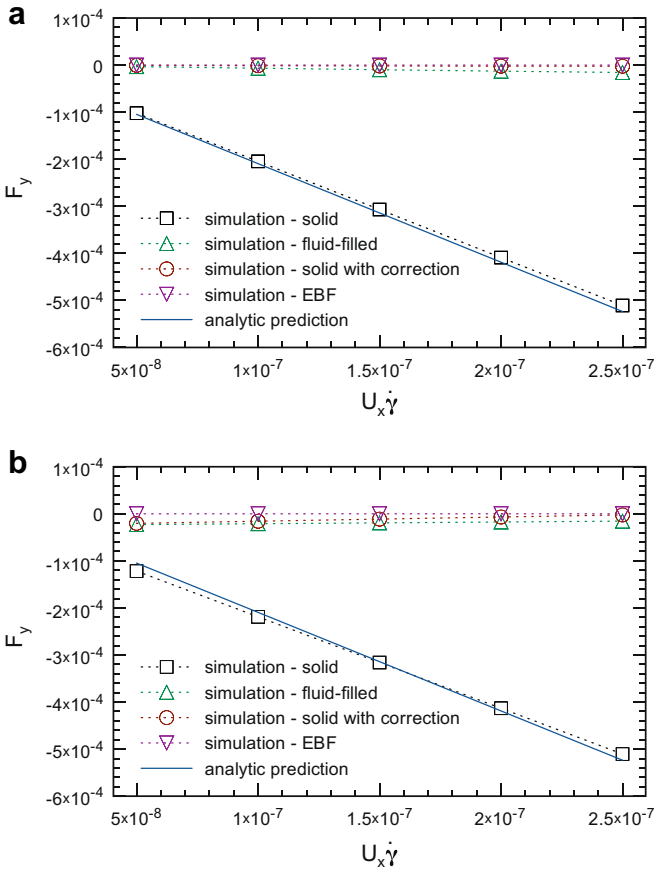

Fig. 5. Force error for sphere suspended in simple shear. In (a), the translational velocity is constant at 0.01, and the shear rate is changed. In (b), the translational velocity is varied while the shear rate is held constant at 2.5×10^{-5}.

4. Conclusions

In this paper, the effect of a moving reference frame was studied for the lattice-Boltzmann method, with a focus on how Galilean errors in the bounce-back boundary condition affect particle dynamics and rheology calculations in sheared suspensions. First, a link-wise error term was derived by considering a fully relaxed system, and this error term was shown to scale as u^2. Next, the link-wise error was extended to surface integrals to calculate errors in force and stresslet. Corrections to reduce the error were proposed, and simulations were performed to validate the calculations.

In the vast majority of cases, the effect of Galilean errors are negligible in terms of particle dynamics and stresslet calculations. In fact, fluid-filled shells show no errors in dynamics, as the internal fluid exactly cancels the link-wise error. However, in quantities dependent on external traction vectors such as normal stress differences in suspensions, magnitudes are exceedingly small, and these Galilean errors may be significant. Also, cases sensitive to particle trajectory may be influenced through the drift induced by the errors in particle force for solid particles. The use of the proposed correction can eliminate these errors and allow more sensitive resolutions of rheological properties.

References

Aidun, C., Lu, Y., 1995. Lattice Boltzmann simulation of solid particles suspended in fluid. J. Stat. Phys. 81, 49–61.

Aidun, C., Lu, Y., Ding, E., 1998. Direct analysis of particulate suspensions with inertia using the discrete Boltzmann equation. J. Fluid Mech. 373, 287–311.

Batchelor, G., 1970. The stress system in a suspension of force-free particles. J. Fluid Mech. 41, 545–570.

Batchelor, G., Green, J., 1972. The determination of the bulk stress in a suspension of spherical particles to order c^2. J. Fluid Mech. 56, 401–427.

Caiazzo, A., Junk, M., 2008. Boundary forces in lattice Boltzmann: analysis of momentum exchange algorithm. Comput. Math Appl. 55, 1415–1423.

Ding, E., Aidun, C., 2003. Extension of the lattice-Boltzmann method for direct simulation of suspended particles near contact. J. Stat. Phys. 112, 685–708.

Einstein, A., 1906. Zur theorie der brownschen bewegung. Ann. Phys. (Leipzig) 19, 371–381.

Heemels, M., Hagen, M., Lowe, C., 2000. Simulating solid colloidal particles using the lattice-Boltzmann method. J. Comput. Phys. 164, 48–61.

Junk, M., Klar, A., Luo, L., 2005. Asymptotic analysis of the lattice Boltzmann equation. J. Comput. Phys. 210, 676–704.

Krieger, I., Dougherty, T., 1959. A mechanism for non-Newtonian flow in suspensions of rigid spheres. J. Rheol. 3, 137–152.

Kulkarni, P., Morris, J., 2008. Suspension properties at finite Reynolds number from simulated shear flow. Phys. Fluids 20, 040602.

Ladd, A., 1994a. Numerical simulations of particulate suspensions via a discretized Boltzmann equation. Part 1. Theoretical foundation. J. Fluid Mech. 271, 285–309.

Ladd, A., 1994b. Numerical simulations of particulate suspensions via a discretized Boltzmann equation. Part 2. Numerical results. J. Fluid Mech. 271, 311–339.

Ladd, A., Verberg, R., 2001. Lattice-Boltzmann simulations of particle-fluid suspensions. J. Stat. Phys. 104, 1191–1251.

MacMeccan, R., 2007. Mechanistic effects of erythrocytes on platelet deposition in coronary thrombosis. Ph.D. thesis, Georgia Institute of Technology.

MacMeccan, R., Clausen, J., Neitzel, G., Aidun, C., 2009. Simulating deformable particle suspensions using a coupled lattice-Boltzmann and finite-element method. J. Fluid Mech. 618, 13–39.

Nguyen, N., Ladd, A., 2002. Lubrication corrections for lattice-Boltzmann simulations of particle suspensions. Phys. Rev. E 66, 046708.

Phung, T., Brady, J., Bossis, G., 1996. Stokesian dynamics simulation of Brownian suspensions. J. Fluid Mech. 313, 181–207.

Sierou, A., Brady, J., 2002. Rheology and microstructure in concentrated noncolloidal suspensions. J. Rheol. 46, 1031–1056.

Sierou, A., Brady, J., 2004. Shear-induced self-diffusion in non-colloidal suspensions. J. Fluid Mech. 506, 285–314.

Singh, A., Nott, P., 2003. Experimental measurements of the normal stresses in sheared Stokesian suspensions. J. Fluid Mech. 490, 293–320.

Wu, J., Aidun, C., in press. Simulating 3D deformable particle suspensions using lattice Boltzmann method with discrete external boundary force.

Zarraga, I., Hill, D., Leighton, D., 2000. The characterization of the total stress of concentrated suspensions of noncolloidal spheres in Newtonian fluids. J. Rheol. 44, 185–220.